EPA-650/2-74-020
January 1974
Environmental Protection Technology Series

FEASIBILITY STUDY OF THE USE OF RESONANCE SCATTERING FOR THE REMOTE DETECTION OF SO_2

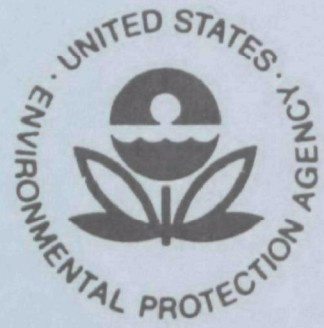

Office of Research and Development
U.S. Environmental Protection Agency
Washington, DC 20460

EPA-650/2-74-020

FEASIBILITY STUDY OF THE USE OF RESONANCE SCATTERING FOR THE REMOTE DETECTION OF SO_2

Prepared by:

Michael C. Fowler and Paul J. Berger

United Aircraft Research Laboratories
East Hartford, Connecticut 06108

Contract No. 68-02-0656
Program Element No. A11010

Project Officer: William F. Herget

Chemistry and Physics Laboratory
National Environmental Research Center
Research Triangle Park, N. C. 27711

Prepared for

OFFICE OF RESEARCH AND DEVELOPMENT
U.S. ENVIRONMENTAL PROTECTION AGENCY
WASHINGTON, D.C. 20460

January 1974

This report has been reviewed by the Environmental Protection Agency and approved for publication. Approval does not signify that the contents necessarily reflect the views and policies of the Agency, nor does mention of trade names or commercial products constitute endorsement or recommendation for use.

ABSTRACT

FEASIBILITY STUDY OF THE USE OF RESONANCE SCATTERING FOR THE REMOTE DETECTION OF SO_2

An analytical and experimental investigation has been carried out to determine the feasibility of using the scattering of ultraviolet radiation by SO_2 as a probe of the concentration of that molecule in stationary source emissions. Both ordinary fl resecence and resonant Raman scattering were considered and experimentally it was found that the latter component was present in the scattered radiation with sufficient magnitude to reduce significantly the degrading effect that ordinary fluorescent quenching has on this scattering technique. Further analysis revealed that current state-of-the-art dye lasers deliver sufficient ultraviolet pulse energy to permit SO_2 concentration determination in practical situations but that fluorescent scattering from particulates presents a possible constraint to the validity of this technique. A field program is recommended to investigate the latter.

TABLE OF CONTENTS

ILLUSTRATIONS

TABLE

SUMMARY

An investigation has been carried out to determine the feasibility of the use of light scattering for the detection of SO_2 in stationary source emissions. An important question concerning the validity of this detection scheme as an SO_2 concentration probe concerns the possibility of whether the detected scattered signal is affected by the concentration of components in the mixture other than SO_2. Fluorescent scattering is particularly vulnerable to this, due to quenching through intermolecular collisions. In contrast, Raman scattering, though ordinarly small in magnitude, is absolutely free of quenching effects and may be enhanced by the occurrence of the phenomenon known as resonant Raman scattering. Measurements were taken at room temperature of the intensity of the light scattered inelastically from an incident laser beam of wavelength 3000 $\mathring{A}$, coincident with an SO_2 absorption peak. The pressure dependence of this signal indicated the presence of an unquenched component of magnitude sufficient to reduce significantly the composition dependence of the SO_2 concentration inferred from a light scattering measurement, as well as to increase the magnitude of the radiation scattered at one atmosphere pressure. Measurements taken at 200°C also indicated the presence of the Raman component, but no information was attained as to whether the magnitude the component depended on the temperature; nor was any information attained as to to whether the magnitude of the Raman component displays a significant sensitivity to which SO_2 absorption peak is coincident with the incident laser radiation wavelength. However, the most serious limitation on this method of SO_2 concentration measurement may be broadband fluorescent scattering from particulates present in the plume, giving rise to the need offer direct field evaluation of this technique.

SECTION I INTRODUCTION

This study is concerned with the feasibility of using the intensity of light scattered inelastically from a laser beam incident on a gas sample containing SO_2 as a valid indicator of the concentration of SO_2 in that gas sample. Particular focus is placed upon the effects of quenching collisions upon the magnitude of the scattered signal. Fluorescent scattering is particularly vulnerable to quenching, and the SO_2 concentration inferred from the scattered light may be significantly influenced by the relative concentrations of the other components in the mixture. In contrast, Raman scattering is immune to quenching effects, but is generally much smaller in magnitude than fluorescence. However, if the wavelength of the incident light lies near an SO_2 absorption line, the magnitude of the Raman scattering cross section may be considerably enhanced. Accordingly, effort was concentrated upon determining whether a Raman component of significant magnitude appeared in the scattered radiation for a laser beam of wavelength identical to that of the SO_2 G line.

Section II presents a brief theoretical background on the phenomena of fluorescent and Raman scattering. Particular emphasis is placed upon the influence of quenching on fluorescent scattering and upon the resonant Raman effect. An expression is developed for the influence of quenching gas pressure on a scattered signal containing both fluorescent and Raman components.

In Section III the experimental apparatus and procedure are described, and the measurements of the dependence of the measured scattered intensity on quenching gas pressure and laser line wavelength are presented and discussed. These measurements indicate the presence in the scattered signal of a Raman component of magnitude sufficient to significantly decrease the dependence of the scattered signal to the quenching gas mixture composition, and increase the magnitude of the signal at atmospheric pressure.

Section IV contains recommendations, based on the results of this study, on the influence of SO_2 concentration and sample to laser distance upon the magnitude of the laser pulse needed to detect that concentration. In addition, areas in which further laboratory scale studies are necessary are enumerated, and a field evaluation program is described.

SECTION II THEORETICAL BACKGROUND

A. Introduction

In this section, the theory underlying the detection of SO_2 by light scattering techniques in the ultraviolet region of the spectrum is briefly reviewed. Part B of this section deals with the detection of SO_2 through fluorescence, a two-photon process wherein the SO_2 molecule first absorbs a photon from the incident laser radiation, and after a short but finite time interval, emits a second photon at a wavelength not necessarily identical to that of the incident radiation. The effect of intermolecular collisions which act to quench or diminish the efficiency of this process is discussed and the resulting limitations on the accuracy of SO_2 concentration determination imposed by quenching are noted. In Part C, detection of SO_2 by Raman scattering, a single photon process free of quenching effects, is discussed with special emphasis placed on enhancement of this process for laser radiation whose wavelength coincides with a maximum in the SO_2 absorption spectrum. Finally, Part D presents the development of an expression, to be used subsequently in analyzing the experimental results, for the pressure variation of the apparent fluorescence quenching rate observed when both fluorescence and Raman scattering are present.

B. Detection of SO_2 by Ultraviolet Fluorescence

Absorption Coefficient

The wavelength dependence of the absorption coefficient of SO_2 in the wavelength region between 2000 $\mathring{A}$ and 4000 $\mathring{A}$ is shown in Fig. 1 (Ref. 1). Three distinct absorption systems are evident. In the wavelength region between 3500 $\mathring{A}$ and 4000 $\mathring{A}$, the absorption is due to excitation of the molecule from the ground or $\tilde{X}$ state to the $\tilde{a}$ state. The latter is a triplet electron spin state whereas the $\tilde{X}$ state is singlet, and radiative transitions between the two are thus rather weak as reflected by the small value of the absorption coefficient. Stronger absorption systems

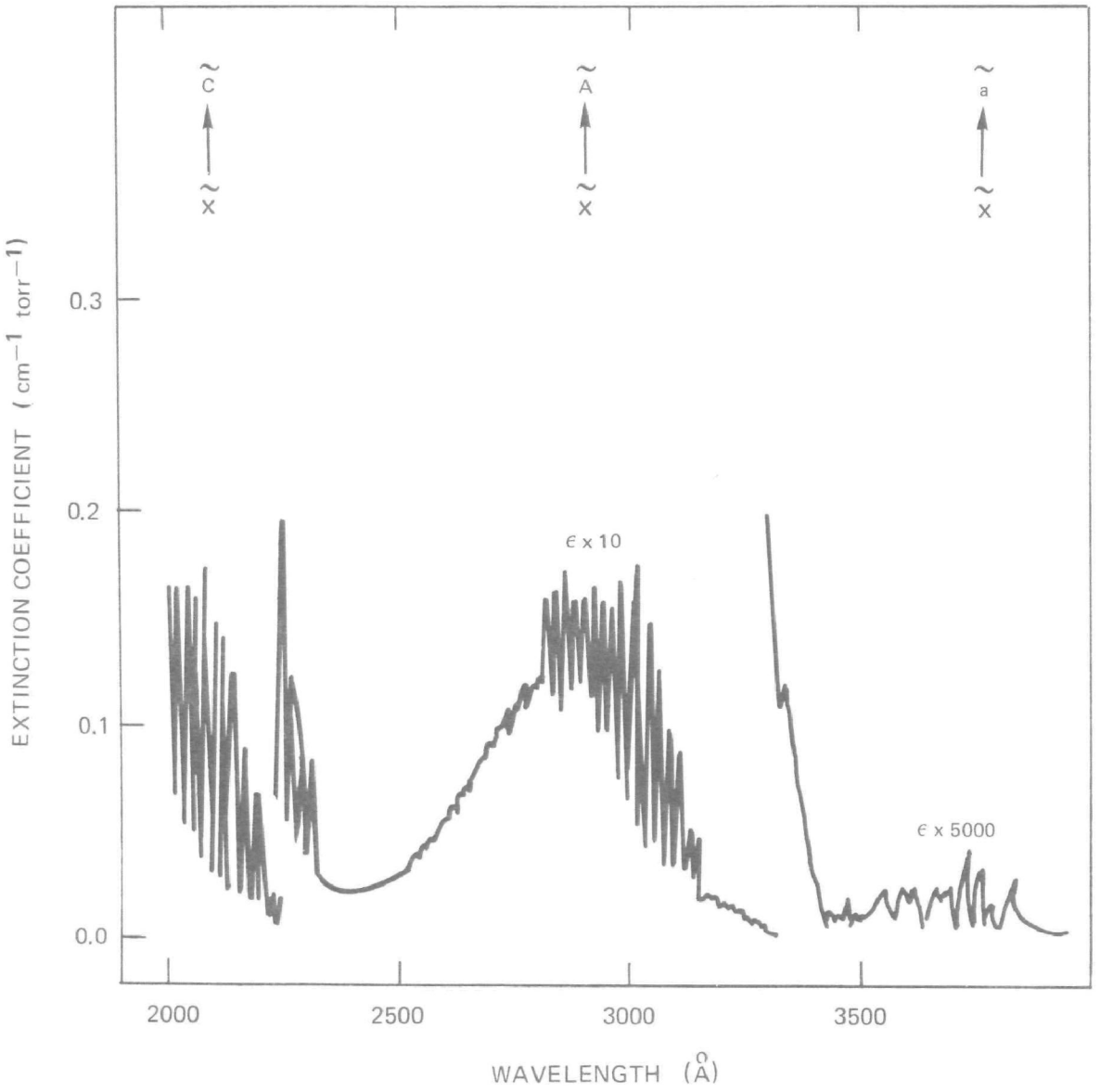

FIGURE 1. WAVELENGTH DEPENDENCE OF THE EXTINCTION COEFFICIENT OF SO_2 FOR THE WAVELENGTH REGION BETWEEN 2000 Å AND 4000 Å

between the ground state and the singlet spin states designated $\tilde{A}$ and $\tilde{C}$ occur in the wavelength regions between 2600 Å and 3400 Å, and 1800 Å and 2400 Å, respectively, and the former of these two systems is the one of interest to this study. The absorption coefficient for all three of these transitions exhibits considerable variation in magnitude. In particular, the $\tilde{X} \rightarrow \tilde{A}$ absorption is seen to consist of many maxima, each of which is several angstrom units wide. The cause of this structure may be seen by examination of Figure 2(a), which presents the variation of the internuclear potential energy V(r), on the internuclear distance r for two electronic energy states of a simple diatomic molecule. The two states are labeled $\tilde{X}$ and $\tilde{A}$, and the potential energy minimum of the upper state is seen to occur at a larger value of r than that of the lower state. The vibrational levels of the upper and lower states are labelel v' and v'', respectively. The probability of a transition occurring between the v'' vibrational level of the lower state to the v' level of the upper with absorption of radiation is proportional to the Franck-Condon factor given by

$$q_{v'v''} = \left[\int_{-\infty}^{\infty} \psi_{v'} \psi_{v''} \, dr\right]^2$$

where $\psi_{v'}$ and $\psi_{v''}$ are the vibrational wave functions of the upper and lower states, respectively. Generally, $q_{v'v''}$ is largest for those values of v' and v" for which $\psi_{v'}$ and $\psi_{v''}$ both have maxima at the same value of r (Ref. 2). For the lowest vibrational level of any given electronic state, the maximum falls at the value of r for which the potential energy curve for the electronic state is at its minimum. But as v' increases, the maxima in ψ_v tend increasingly to occur at the values of r for which the potential energy curve equals the energy of the vth level. During a transition between two electronic states, the value of r is constant, since the time elapsed during the transition is much shorter than the vibrational period of the two nuclei. A transition from v'' = 0 in the $\tilde{X}$ state is thus shown as a vertical arrow in Figure 2 and, from the argument given above, the frequency dependence of the absorption coefficient for transitions originating from this level will consist

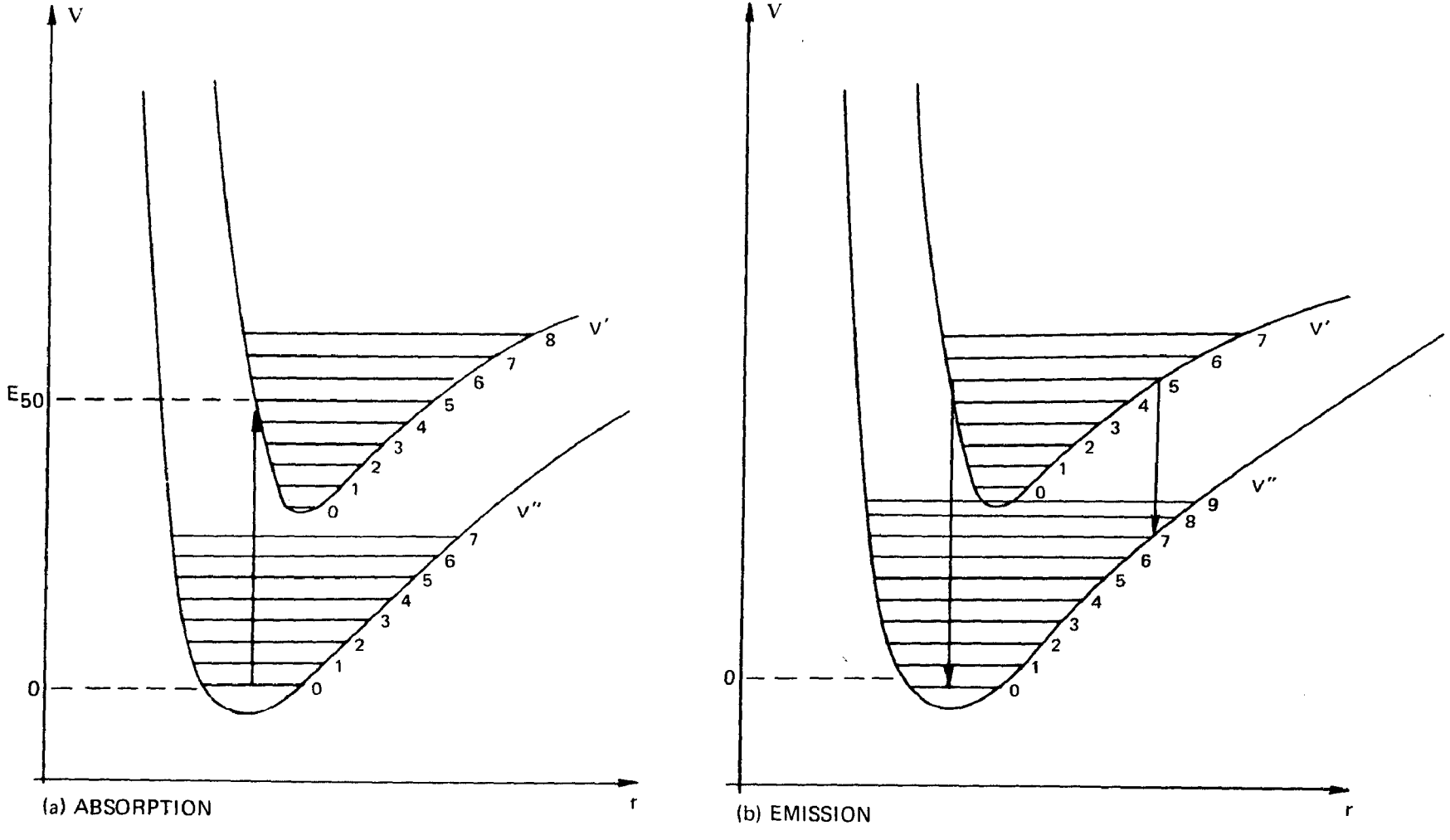

FIGURE 2. VIBRATIONAL STRUCTURE OF ELECTRONIC TRANSITIONS

of a series of maxima the largest of which lies at a frequency equal to E_{50}/h, where h is Planck's constant, and E_{50} is, as indicated in the figure, the energy of the level v' = 5 relative to that for v'' = 0. The frequency between the maxima will be approximately $\Delta E'/h$ where $\Delta E'$ is the vibrational energy constant of the upper level. Since the diatomic molecule also has one rotational degree of freedom, each of the maxima mentioned above will display rotational fine structure whose character will depend on the nature of the electronic states $\tilde{X}$ and $\tilde{A}$ (Ref. 3). In contrast to the simple situation depicted in Figure 2, the portrayal of the vibrational potential energy of each electronic state of SO_2 is much more complicated. As shown in Figure 3, SO_2 has three normal vibrations, and the vibrational potential energy of any given electronic state is seen to be dependent on the sulphur-oxgyen bond distances, as well as the angle between these bonds. The structure shown in Figure 1 for the $\tilde{X} \rightarrow \tilde{A}$ transition has been attributed to transitions from the lowest energy levels of the first two normal modes shown in Figure 3 to excited levels of these modes in the $\tilde{A}$ electronic state (Ref. 4). In addition, it is noted that SO_2 has three rotational degrees of freedom, giving rise to a very dense and complicated rotational fine structure in the $\tilde{X} \rightarrow \tilde{A}$ absorption spectrum which in turn causes the observed width of several angstrom units in each of the maxima shown in Figure 1.

Unquenched Fluorescent Emission

Examination of Figure 2(b) reveals how the frequency distribution of fluorescent emission is determined by the properties of the electronic molecular states involved. Generally, photon emission occurs prior to vibrational relaxation of the molecule in the excited state (Ref. 5). Accordingly, for the case shown in Figure 2, the molecule, once excited to v' = 5 by absorption of a photon of energy E_{50} will most probably emit a photon with energy E_{50} or E_{57}, and transitions at energies of E_{56} and E_{58} will be only slightly less probable than that with energy E_{57}. Therefore, the frequency distribution of fluorescent intensity observed from a sample of gas irradiated with photons of energy E_{50} will exhibit one maximum at

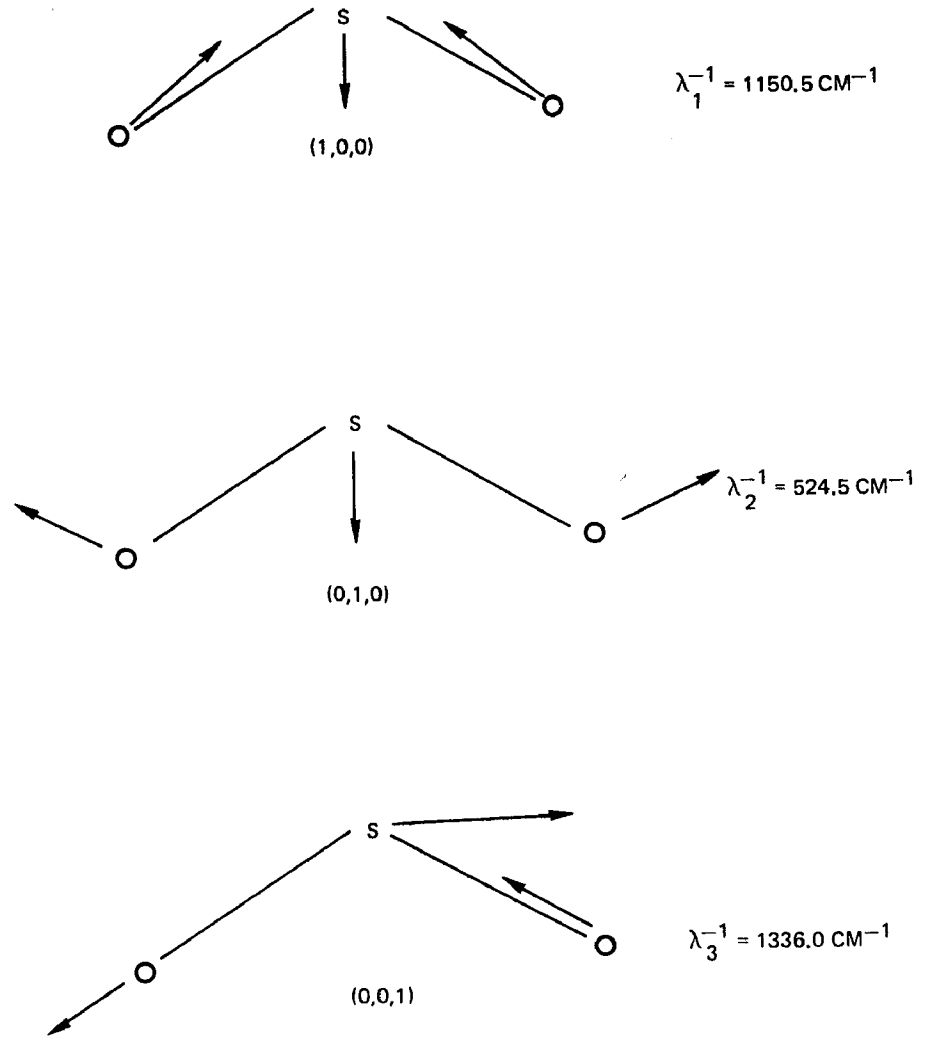

FIGURE 3. THE NORMAL VIBRATIONS OF SO_2

E_{50}/h, corresponding to resonance fluorescence, and other maxima centered around E_{57}/h. Figure 4 illustrates the wavelength distribution for fluorescence from SO_2 pressure at 0.01 torr, and the fluorescence intensity distribution exhibits properties qualitatively similar to those described above for the simple example shown in Figure 2. The wavelengths for the two maxima observed below 3800 Å are unshifted as the SO_2 pressure was increased from 0.01 torr to 0.5 torr, indicating that vibrational relaxation of the $\tilde{A}$ state prior to photon emission is unimportant and that the observed fluorescent intensity distribution is determined by spectroscopic rather than gas kinetic properties of the SO_2 molecule in the $\tilde{A}$ state in this pressure range (Ref. 5).

Quenched Fluorescent Emission

However, the absolute intensity of the $\tilde{A} \rightarrow \tilde{X}$ fluorescence was observed to decrease as the SO_2 pressure was increased to 0.5 torr, and fluorescence from the $\tilde{a}$ state at wavelengths greater than 3900 Å was observed as indicated in Figure 4. These facts indicate that quenching of the $\tilde{A}$ state by SO_2 occurs, leaving the molecule in the $\tilde{a}$ state, for SO_2 pressures comparable to those found in coal-fired power plant effluents. Other molecules are also effective in quenching both the $\tilde{A}$ and $\tilde{a}$ states of SO_2. The quenching rate coefficients for some of these are given in Table 1 along with radiative decay rates for the $\tilde{A}$ and $\tilde{a}$ state.

The results given in Table 1 reveal that the rate of quenching of SO_2 at the $\tilde{A}$ state is quite sensitive to the identity of the quenching molecule and raises the question as to whether, for a fixed quantity of SO_2 in a gaseous mixture, the observed fluorescent signal is sensitive to the relative amounts of the other components in the mixture. In the following discussion the expression is developed for the magnitude of the observed signal from a fixed pressure of SO_2 gas as a function of the amount of quenching gas added to the sample. It is assumed that the pressure of SO_2 in the sample is low enough that the degree of attenuation of the incident laser radiation is negligible. For the situation where the rate of destruction of excited state SO_2 by radiative decay and quenching collisions

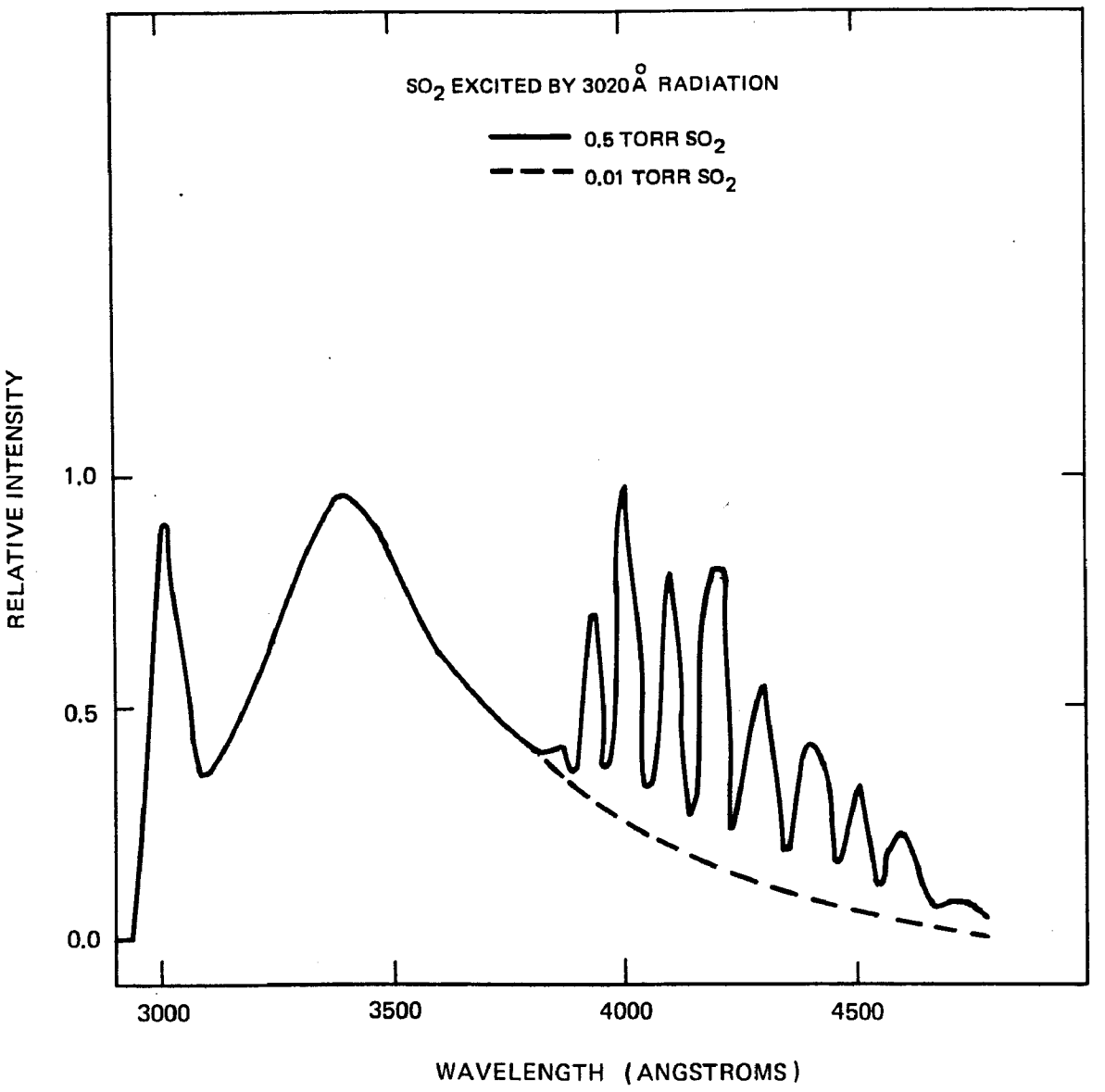

FIGURE 4. WAVELENGTH DEPENDENCE OF FLUORESCENCE OF SO_2 FOR THE WAVELENGTH REGION BETWEEN 2900 Å AND 5000 Å

TABLE 1. QUENCHING RATES OF SO_2 ULTRAVIOLET RADIATION

($\tilde{A} \longrightarrow \tilde{X}$)
(RADIATIVE DECAY RATE = 2.4×10^4 SEC^{-1})

QUENCHING MOLECULE	QUENCHING RATE (SEC^{-1} $TORR^{-1}$)	REFERENCE
CO_2	8.0×10^5	8
	7.1×10^6	6
NO	5.5×10^6	6
N_2	2.7×10^6	6
CO	3.1×10^6	6
D_2O	1.8×10^7	6
O_2	2.5×10^6	6
SO_2	8.7×10^6	6
	5.1×10^6	8

is fast compared to the temporal variation of the incident laser intensity, the rate of production of excited state SO_2 is balanced by the rate of decay of SO_2 from the excited state

$$\phi_o \alpha p_{SO_2} - N^* \left(\sum_i k_i p_i + r_r\right) = 0 \qquad (1)$$

where ϕ_o is the incident laser flux, α is the SO_2 absorption coefficient, assumed to be unaffected by pressure, p_{SO_2} the SO_2 pressure, N^* the SO_2 excited state number density, k_i the quenching coefficient of component i at pressure p_i, and r_r is the radiative decay rate of SO_2. The observed fluorescence intensity, I, is given by the product of κ, the experimental detection efficiency, and $h\nu_f N^* r_r$ where $h\nu_f$ is the energy per photon of the fluorescence. The ratio of the fluorescence intensity, I_o, observed in the absence of all quenching gases other than SO_2, to that observed when a quenching gas is present at pressure p_q is given by

$$I_o/I = \frac{k_{SO_2} p_{SO_2} + k_q p_q + r_r}{k_{SO_2} p_{SO_2} + r_r} \qquad (2)$$

and a plot of I_o/I is linear with p_q with a slope m equal to

$$m = \frac{k_q}{k_{SO_2} p_{SO_2} + r_r} . \qquad (3)$$

If the quantities k_{SO_2} and r_r are known, the quantity k_q can be obtained from a plot of I_o/I vs p_q. Conversely, if all the quenching coefficients k_i are known, it is possible to calculate the sensitivity of I/I_o^o, the fluorescent efficiency or fraction of absorbed radiation emitted as fluorescence,

$$\frac{I}{I_o^o} = \frac{r_r}{r_r + \sum_i k_i p_i} , \qquad (4)$$

to the composition of the gas mixture.

Using the information summarized in Table 1, the calculated value of I/I_o^o is 6.2×10^{-6} for a trace of SO_2 in a one atmosphere mixture containing 77% N_2, 12% CO_2, 8% H_2O and 3% O_2, a mixture typical of the exhaust from an oil flame. In contrast, the fluorescence efficiency is decreased by 30% from the above amount if the water fraction is increased to 20% and the fractions of the other components relative to one another are held constant. Thus, the detected SO_2 fluorescence signal can be significantly influenced by the composition of the mixture sampled. In addition it is noted that the results presented in Table I are for a mixture temperature of 300°K. Whether the fluorescent efficiency of a given gas mixture is sensitive to gas temperature can therefore not be determined from the data in Table I and remains a serious question as to the validity of fluorescent emission as a means of detecting SO_2.

C. Raman Scattering

In the previous section the process of fluorescent scattering of radiation was briefly reviewed. It was seen that fluorescent scattering is essentially a two-photon process, involving first the excitation of the molecule from the ground to the excited state by absorption of a photon from the incident radiation field, followed, after a time interval determined by the radiative characteristics of the excited state, by photon emission, leaving the molecule in a lower energy state. It was seen that due to the finite time interval spent in the excited state, collisional quenching becomes a significant alternate to photon emission as a decay channel from the excited state and thereby compromises the validity of fluorescent scattering as an accurate measure of SO_2 concentration. In this section it will be shown briefly that in contrast to fluorescent scattering, the Raman effect occurs only while the molecule is in the electric field of the incident photon, thereby being a one-photon process and free of quenching effects. It will also be indicated how the magnitude of the Raman scattered signal can become greatly enhanced if the incident radiation wavelength coincides with that of a maximum in the absorption spectrum of the molecule.

Nature of the Raman Effect

The nature of the Raman effect can be simply understood by considering the oscillating electric field associated with a photon flux incident on a molecule and the perturbing effect that this field has upon the wave functions associated with molecule energy levels (Ref. 7). As a result of the interaction between the electric field and the molecule, photons are scattered inelastically out of the incident flux and their frequency of oscillation either decreased, if energy is transferred to the molecule, or increased if energy is transferred from the molecule to the field. The intensity of radiation scattered per unit beam path, per molecule at frequency ν_s is given in terms of the incident intensity, I_o, by the following expression

$$I = \frac{128\,\pi^5\, I_o \nu_s^4}{9\, c^4\, h^2} \sum_{\sigma'} \left| \hat{E}_{\sigma'} \cdot \vec{P}_{n'n} \right|^2 \qquad (5)$$

where

$$\vec{P}_{n'n} = \sum_{n''} \frac{\vec{M}_{n'n''}(\hat{E}\cdot\vec{M}_{n'n''})}{\nu_{n''n} - \nu} + \frac{(\hat{E}\cdot\vec{M}_{n'n''})\,\vec{M}_{n''n}}{\nu_{n''n'} + \nu}$$

where ν is the frequency of the incident radiation, n and n' represent the initial and final states of the molecule, n'' represents states other than the initial and final ones, and $\hat{E}_{\sigma'}$ and $\hat{E}$ are, respectively, unit vectors for the polarization state σ' and the incident electric field. In the case of interest here the states denoted by n and n' are the lowest and first excited vibrational levels, respectively, of the ground electronic state of the molecule in which case ν_s is given by $\nu - E_v/h$ where E_v is the vibrational energy difference between the states n and n'. The states n'' are the vibrational levels of the excited electronic states of the molecule, the quantity $M_{n''}$ is the electric dipole operator matrix element and $h\nu_{n''n}$ is the energy difference between the levels n'' and n. From the above expression it is seen that the fraction of the beam scattered with frequency ν_s is related to the sum of the strengths of all optical transitions involving the states n' and n.

In particular, when the value of ν is nearly identical to that of an optically allowed transition the phenomenon is referred to as resonance Raman scattering and the scattered intensity is given by

$$I_{res} = \frac{128\,\Pi^5\, I_o \nu_s^4}{9\, c^4\, h^2} \quad \frac{|M_{n'n''}|^2\, |M_{n''n}|^2}{(\nu_{n''n} - \nu)^2 + d_{n''}^2} \tag{6}$$

where $d_{n''}$ is the line width of the allowed absorption line. Behringer (Ref. 9) points out the near equality between the above expression and that for the intensity of radiation absorbed in an allowed optical transition provided that $d_{n''}$ is determined by the radiative decay rate from the level designated by n''. For this situation the magnitude of I_{res} would equal the fluorescent intensity in the absence of quenching collisions in the hypothetical case where only resonant fluorescence could occur. In practice I_{res} is not so large as predicted due most probably to the fact that $d_{n''}$ is determined by factors other than the radiative decay rate and to the breakdown in the validity of the time independent perturbation theory which was used to derive Equation 6 (Ref. 10). Still, resonance Raman scattering has been observed to be quite intense in liquid solution (Ref. 11) as shown in Figure 5. The large number of overtone and combinational lines is characteristic of resonant Raman scattering. The sharpness of the resonant Raman lines in comparison to the rather broad fluorescence is a result of the fact that the Raman effect is a direct scattering process and involves no intermediate energy level from which the absorbed energy can be quenched or reemitted over a wide wavelength interval.

D. Analysis of Scattering Containing Both Raman and Fluorescence Components

In the experiments to be described in Section III, the magnitude of the incident laser signal scattered by a gas sample containing SO_2 and N_2 was measured as a function of the amount of N_2 in the sample. Measurements were taken of the scattered signal intensity at a light frequency which was displaced from that of the incident laser radiation by an amount corresponding to the energy necessary to excite the symmetric stretch vibrational mode of SO_2, 1151 cm^{-1}. The measured

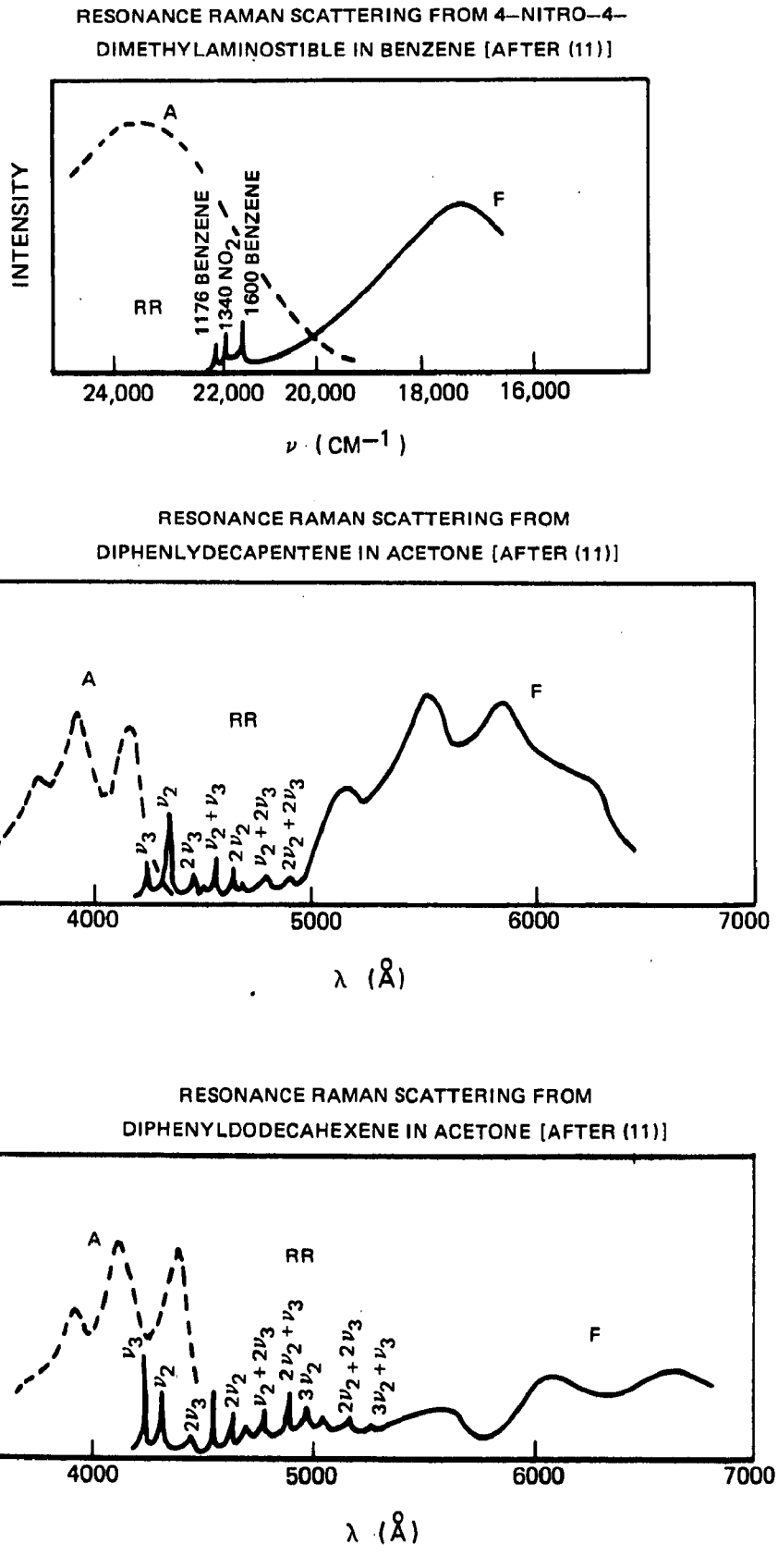

FIGURE 5. RESONANT RAMAN SCATTERING AND FLUORESCENCE IN LIQUID SOLUTIONS

signal is therefore expected to contain both a fluorescent component which, as indicated in Section IIB, is quenched by the addition of N_2 and a Raman component whose intensity is unaltered by N_2 addition. In the following paragraph the expected pressure variation of such a signal is discussed, and it is shown that the observed pressure variation indicates the relative magnitudes of the fluorescent and Raman components of the signal.

Pressure Variation of Scattered Signal

In Section IIB it was shown that the magnitude of the scattered intensity due to fluorescent scattering decreases upon the addition of a gas which quenches the fluorescence, and in Section IIC the immunity of the Raman effect to quenching effects was described. Therefore, the pressure dependence of the observed scattered intensity I, which contains both fluorescence and Raman components, is given by the following expression

$$I = \frac{I_F^o}{1 + Xp_q} + I_R \tag{7}$$

where I_F^o is the magnitude of the fluorescence component in the absence of the quenching gas, p_q is the quenching gas pressure, I_R is the magnitude of the Raman component, and X, the quenching coefficient, is given in terms of quantities defined in Section IIB.

$$X = \frac{k_q}{k_{SO_2} p_{SO_2} + r_r} \cdot \tag{8}$$

If the Raman scattering component is negligible for all values of p_q, the quenching coefficient can be calculated from experimentally measured quantities directly from Equation 7 with I_R set equal to zero, and the result is

$$X = \left(\frac{I_F^o - I}{I} \right) \Big/ p_q . \tag{9}$$

If I_R is indeed zero, X is of course independent of p_q. If, however, I_R is not negligible, the experimentally derived value of X exhibits a pressure dependence and is no longer defined by the simple expression given in Eq. 8. The pressure dependence of the apparent quenching coefficient X_a, derived as above under the assumption that I_R is zero when in fact it is not, is given by the following expression.

$$X_a^{-1} = \frac{I_F^o + I_R}{I_F^o X} + \frac{I_R p_q}{I_F^o} \qquad (10)$$

It is seen that a plot of X_a^{-1} against p_q will yield a straight line whose slope is equal to the ratio of the Raman component of the scattered intensity to that of the fluorescence component unquenched by foreign gas addition. The value of the slope of the curve can then be combined with the value of X_a^{-1} at zero quenching pressure to yield the value of X which in turn is used to obtain k_q if k_{SO_2}, p_{SO_2} and r_r are known. The magnitude of the Raman component relative to that of the fluorescence, I_F, at any value of p_q is given by

$$\frac{I_R}{I_F} = \frac{I_R}{I_F^o}\left(1 + X p_q\right) \qquad (11)$$

If the value of I_R/I_F is large compared to unity at atmospheric pressure, then the scattered light intensity is made up mostly of the Raman component, is free from quenching effects and is thus a mixture composition and perhaps temperature independent indicator of the SO_2 concentration in the mixture.

SECTION III Experimental Results

A. Apparatus

Radiation Source and Optical Train

The laser used in these experiments was the UARL vortex stabilized flashlamp pumped dye laser which has been described in detail elsewhere (Ref. 12). The dye used in these experiments was Rhodamine 6G at a concentration of 140 μ mole/liter and the broadband output of the laser with a fresh dye solution was typically 150 mJ contained in a pulse with a half-width at half-height of 0.75 μsec. Tuning of the device was accomplished by insertion into the cavity of two etalons. One of these etalons was a piece of quartz, one of whose surfaces was coated with two highly reflecting layers separated by 4 μm of dielectric. Its free spectral range was 9 Å at a wavelength of 6000 Å. With these etalons in place, the laser output could be confined to a single line several tenths of an anstrom unit wide over a wavelength range which extended from 5800 Å to 6150 Å. The laser output was focussed onto a crystal of ADP immersed in cylohexane to protect against desication of the crystal. The diverging beam, a portion of which was now at one half the wavelength of the original laser output, was refocussed in the middle of the fluorescence cell, the temperature of which could be varied between ambient and 200°C. after passing through the cell the beam was incident on an RCA 935 photodiode equipped with a low pass filter with a cut off wavelength of 4100 Å. The output of the photodiode was amplified and used to trigger the electronics which will be described later. The entire optical train is drawn schematically in Figure 6, and a detail of the flashlamp-dye cell unit is shown in Figure 7 (Ref. 12). The light scattered by the SO_2 in the gas cell was focussed by a quartz lens onto the entrance slit of a Jarrell Ash 75-150 instrument which could be used either as a monochrometer or a spectrograph with a dispersion of about 8 Å/mm at 3000 Å. The image of the scattering region was rotated by placing an appropriate mirror assembly between the quartz lens and the slit. This was done in order to render the image

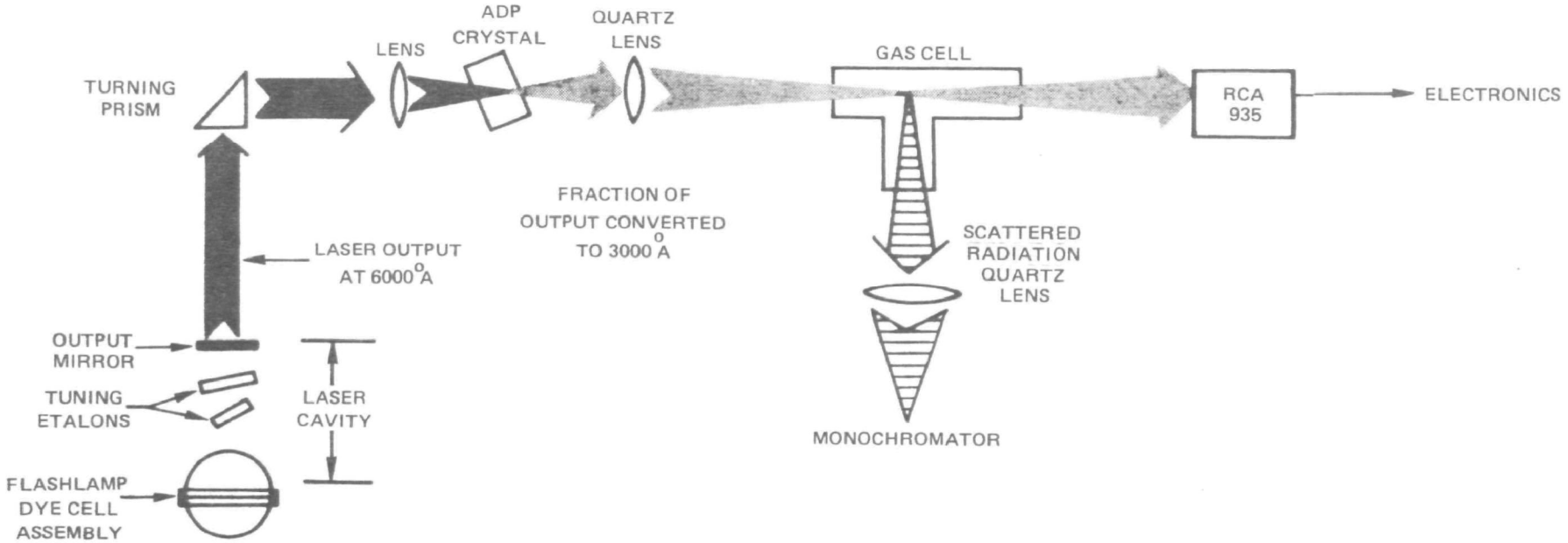

FIGURE 6. OPTICAL TRAIN USED IN SO_2 LIGHT SCATTERING MEASUREMENTS

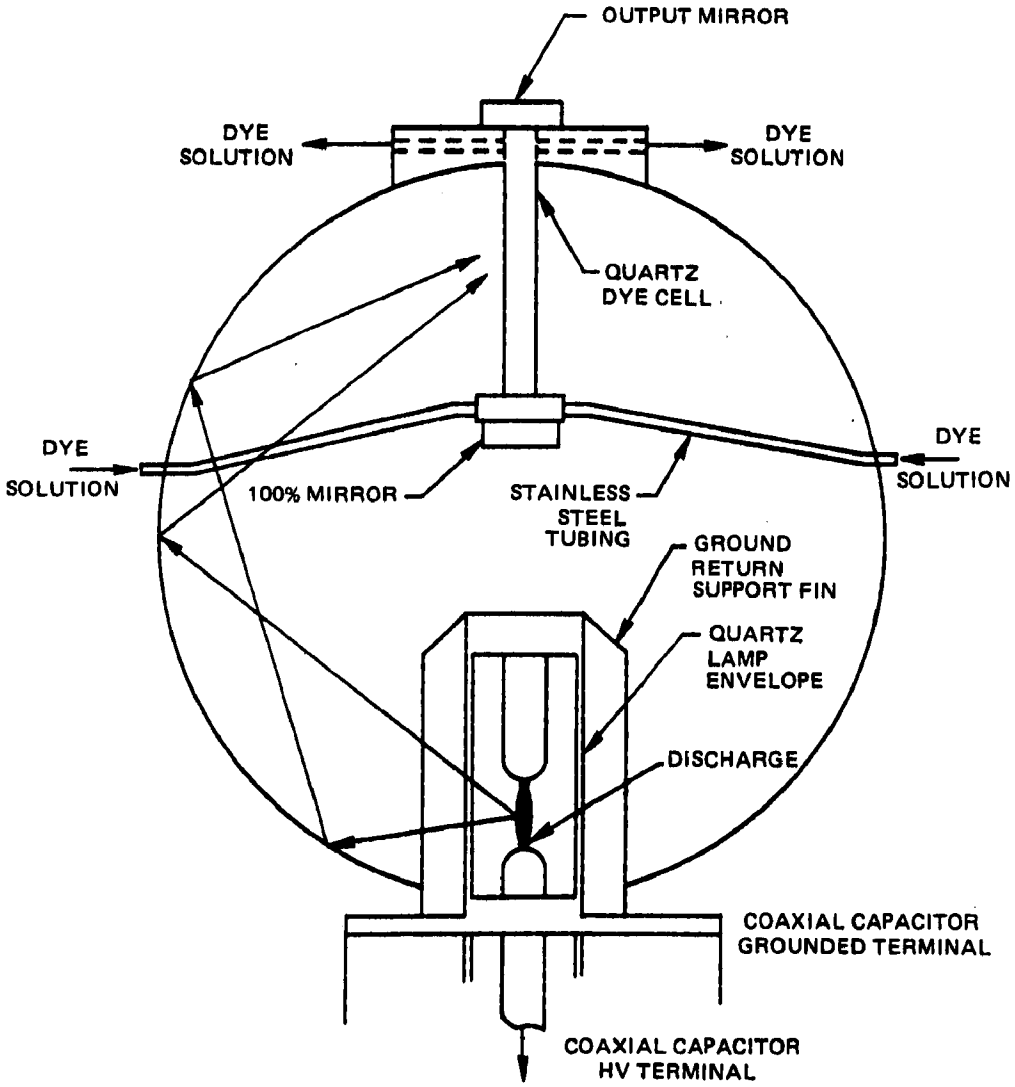

FIGURE 7. 1.2–W FLASHLAMP PUMPED DYE LASER

and the slit parallel, thus increasing the magnitude of the scattering volume accepted by the monochrometer compared to the volume accepted were the image and slit perpendicular to one another. During fluorescence measurements, the monochrometer entrance and exit slits were opened to 3 mm and the throughput of the instrument thus lay over a spectral region 24 Å wide. This throughput impinged on an RCA 8575 photomultiplier equipped with a low-pass filter with a cut-off wavelength of 4100 Å. The photomultiplier output was analyzed in a manner to be described later.

To analyze the spectral properties of the laser output, the latter was deflected onto a strip of scotch tape placed in front of the spectrograph entrance slit, the tape acted as a radiation diffuser and provided uniform illumination of the slit whose width was set to about 0.05 mm for this measurement. The spectrograph throughput was collected on Polaroid Type 52 film and the spectrum from a low pressure mercury vapor germicidal lamp was superimposed on the photograph of the laser output spectrum. The film containing the superimposed spectra was analyzed using a microscope equipped with a movable stage whose position was measureable to within 0.0001 inch. Under magnification, spectral lines appeared as nearly gradient-free grey areas on the photographs. The center wavelength for a given line was associated with the center of the corresponding grey area. The effective dispersion for each spectrogram was calculated from the measured separation between the mercury lines at 2967.28 Å and 3021.50 Å, and the value of this quantity was reproducable to about 0.5%. The chief cause of error in such a measurement is the contribution to the measured width of the mercury line at 3021.50 Å by intensity from a neighboring but less intense, by a factor of 3, line at 3023.48 Å. The wavelength of the laser line was then calculated by combining the measured dispersion of the spectrogram with the measured distance between the laser line and the line at 3021.50 Å. The error in the position of the line at 3021.5 Å is thus seen to affect both the calculated dispersion and the measured position of the laser line wavelength relative to the 3021.5 Å mercury line. Routine calculation indicates that the calculated value of the laser line wavelength is at worst 0.5 Å too high as a result of this source of

error. The half width of the frequency doubled laser line at one percent of the peak intensity was estimated by these measurements to be about 0.48 Å, which infers a half-width at half-height of 0.22 Å if the line profile is Gaussian.

Electronics

In practice, the intensity of the scattered laser radiation was measured by averaging, over a number of laser pulses, the magnitude of scattered light signal received by the photomultiplier attached to the monochrometer. The following paragraph describes the electronic apparatus employed in obtaining this average.

The electronic instrumentation used in processing the photomultiplier output current consisted of a Burr-Brown SHM 40 sample and hold circuit, a Dymec 2401 A integrating digital voltmeter, which was used as a voltage-to-frequency converter, and a Hewlett Packard 5280 A reversible counter connected as shown in Figure 8. In principle, the sample and hold circuit attains the voltage at its input during the 2 μsec aperture time which is defined by the trigger signal generator which in turn is triggered by the laser pulse. The output of the sample and hold circuit is maintained at the voltage reached by the end of the 2 μsec aperture period, and this voltage is fed to the voltage-to-frequency converter, the output of which is an oscillating voltage whose frequency is proportional to the voltage input. During its 20 msec aperture time, the counter registers the number of times that this oscillating voltage passes through zero and displays this number as its output. The output of the counter is summed over 100 laser pulses and is taken as the measure of the average magnitude of the laser radiation scattered by the SO_2 in the sample cell into the wavelength range as defined by the monochrometer. Typically the maximum output of the photomultiplier was of the order of a volt when no quenching gas was present in the cell and decreased to several millivolts when the quenching gas pressure was one atmosphere. In practice, the sample and hold circuit functions best at voltages of more than 0.1 V, and so provision was made for the insertion of preamplifiers between the photomultiplier tube and the sample and hold circuit. The linearity of the entire electronics assembly was checked and found to be satisfactory.

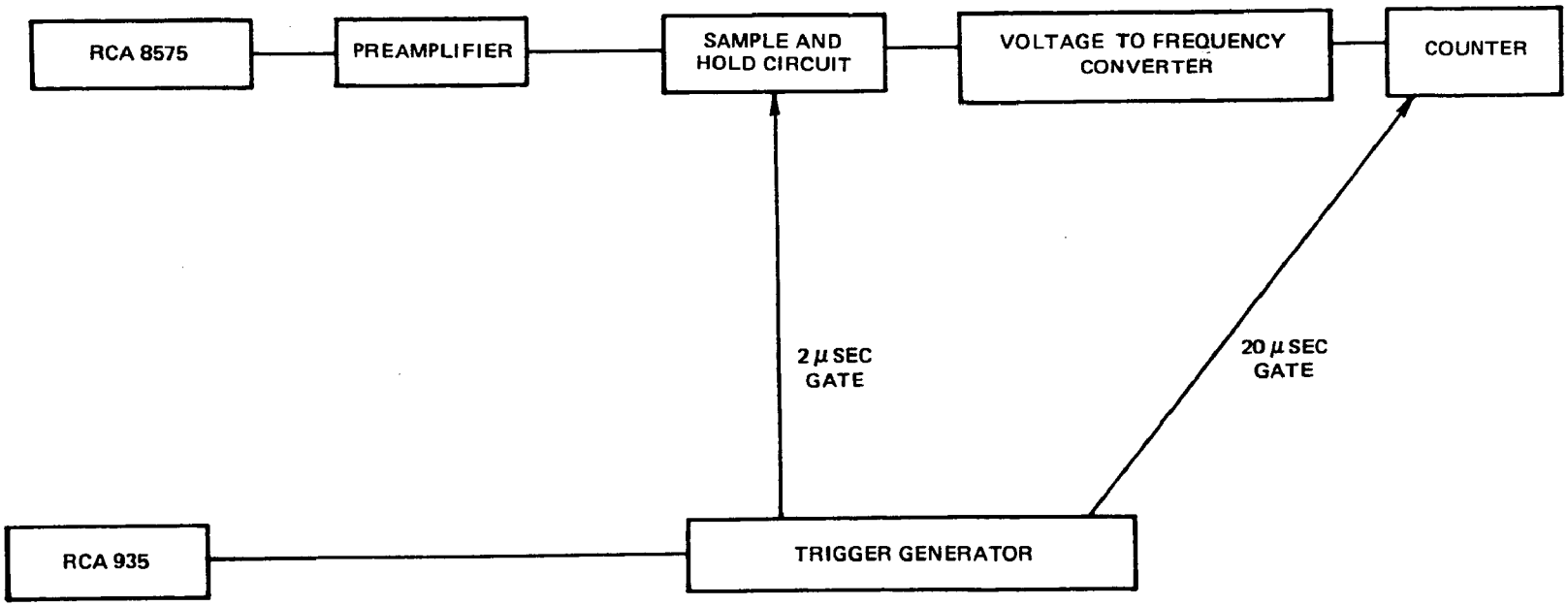

FIGURE 8. ELECTRONICS USED IN SO_2 LIGHT SCATTERING EXPERIMENTS

The maximum photomultiplier anode current was typically less than 100 μa, and sufficient capacitance was added between the last four dynodes to guarantee against any nonlinearity of photomultiplier response to the scattered light intensity. After extensive efforts had succeeded in eliminating extraneous electrical noise generated by the flashlamp and its attendant circuitry, it was found that the pulses constituting the photomultiplier dark current were the main source of background noise and the photomultiplier was operated at 2300 V cathode voltage at which the signal to dark current noise was found to be maximum. The photomultiplier was not cooled although in practice doing so would further lower the dark current.

Gas Handling System

A schematic diagram of the gas handling system used in these experiments is shown in Figure 9. Using the mechanical pump, a base vacuum of 0.02 torr was obtained as indicated by the Hastings-Raydiest 0V6M thermocouple gauge. The pressure of SO_2 added to the cell was measured using a Wallace and Tiernan Mechanical Gauge, labeled #1, in Figure 9, and this pressure was typically less than 0.5 torr. The pressure of N_2 added to the cell was read using the mechanical gauges. In practice, after sufficient SO_2 had been added to the cell, valves 1 and 5 were closed and valves 2 and 3 opened, a vacuum of about 0.03 torr attained, valves 2 and 3 closed and 1 reopened. This procedure was carried out to guarantee against leakage of additional SO_2 into the scattering cell during the course of an experiment.

B. Experimental Procedure and Results

Procedure

The procedure followed in obtaining data was as follows: with the tuning etalons adjusted so as to attain approximately the desired laser output wavelength, 6000 Å, the laser output was maximized by adjusting the orientation and position, relative to the first lens, of the ADP crystal. As a result the frequency doubled output from the crystal was now centered at approximately 3000 Å, nearly coincident

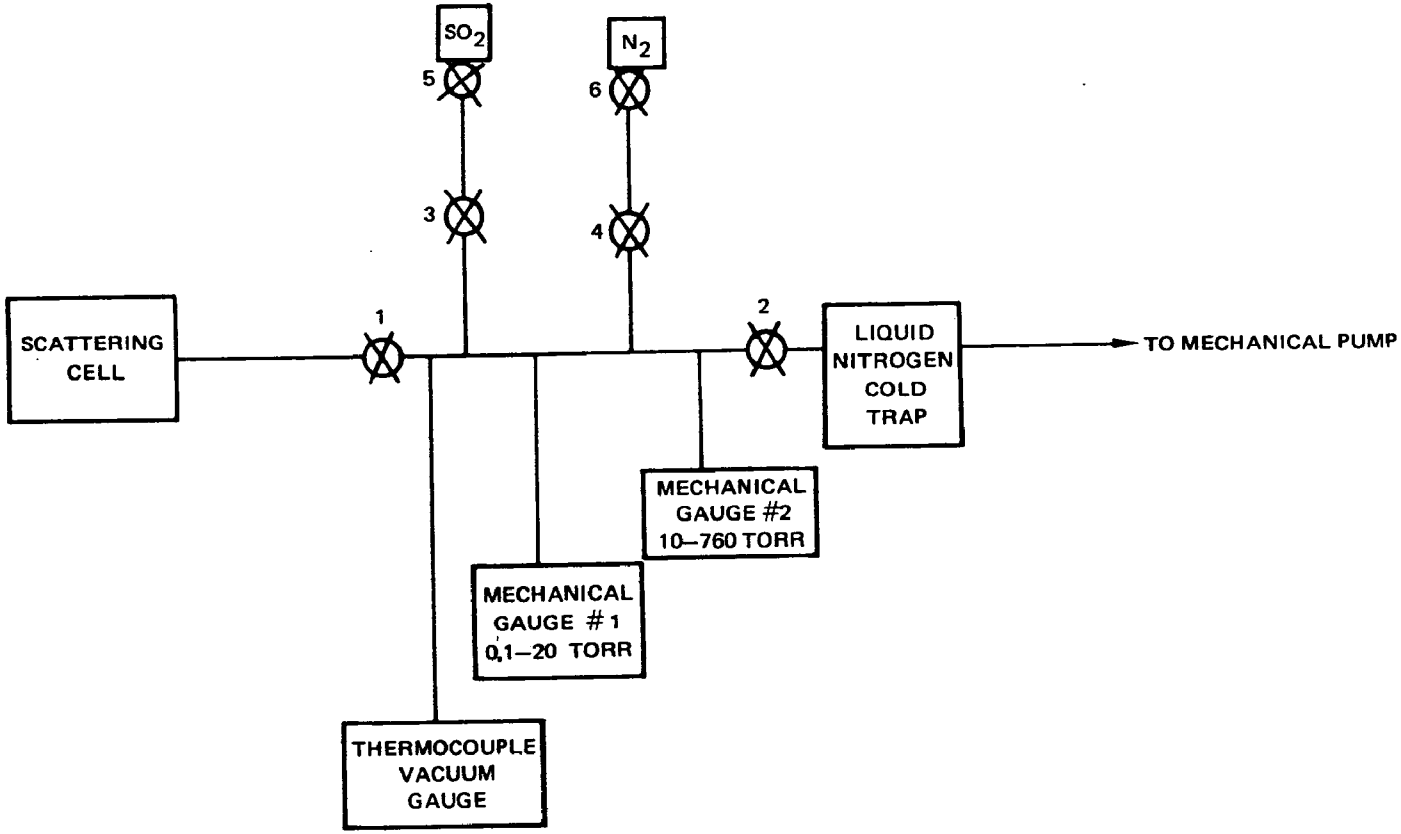

FIGURE 9. GAS HANDLING SYSTEM USED IN SO_2 LIGHT SCATTERING EXPERIMENTS

with the wavelength of the G line in the $\tilde{X} \rightarrow \tilde{A}$ absorption system of SO_2. Spectral scans of the intensity of the radiation scattered from an incident beam at 3000 Å disclosed a sharp maximum at approximately 3105 Å followed by a much broader maximum at 3400 Å. The Stokes component for the symmetric stretch mode of SO_2 appears at 3105 Å for Raman scattered radiation whose original wavelength is 3000 Å. Accordingly, the monochrometer was set at 3105 Å with the exit and entrance slits opened so as to permit radiation 12 Å to either side of this wavelength to pass through the instrument and impinge on the photomultiplier. Sulphur dioxide was admitted to the cell to a pressure between 0.3 and 0.5 torr and the wavelength of radiation incident on the cell was tuned by suitably adjusting the intracavity etalons and the ADP crystal orientation. The degree of coincidence between the wavelength of the incident radiation and the maximum in the SO_2 G line absorption coefficient was judged by the magnitude of the photomultiplier output signal. Runs were taken with varying degrees of coincidence. With the tuning of the laser line completed, measurements were made of the average scattered radiation signal, as well as the average background signal. Both measurements were made for one hundred laser pulses. The average laser pulse output signal was also measured in the same way by measuring the output of the RCA 935 photodiode. The scattered intensity at 3105 $\pm$ 12 Å, I_o, normalized with respect to the laser output is given by

$$I_o = \frac{I_o' - I_B}{I_L} \tag{12}$$

where I_o', I_B and I_L are the measured scattered, background and laser signal, respectively. Nitrogen quenching gas was added to the cell to the desired pressure, the above process was repeated after a fifteen minute pause to allow complete mixing of the N_2 and SO_2, and the expression in Eq. 12 was used to calculate the value of I to be used in Eq. 9. Generally, a complete experimental run consisted of measurements at two or more N_2 pressures, as well as one at zero N_2 pressure. At the end of a run, the wavelength of the laser radiation was determined in the manner described in Section IIIB.

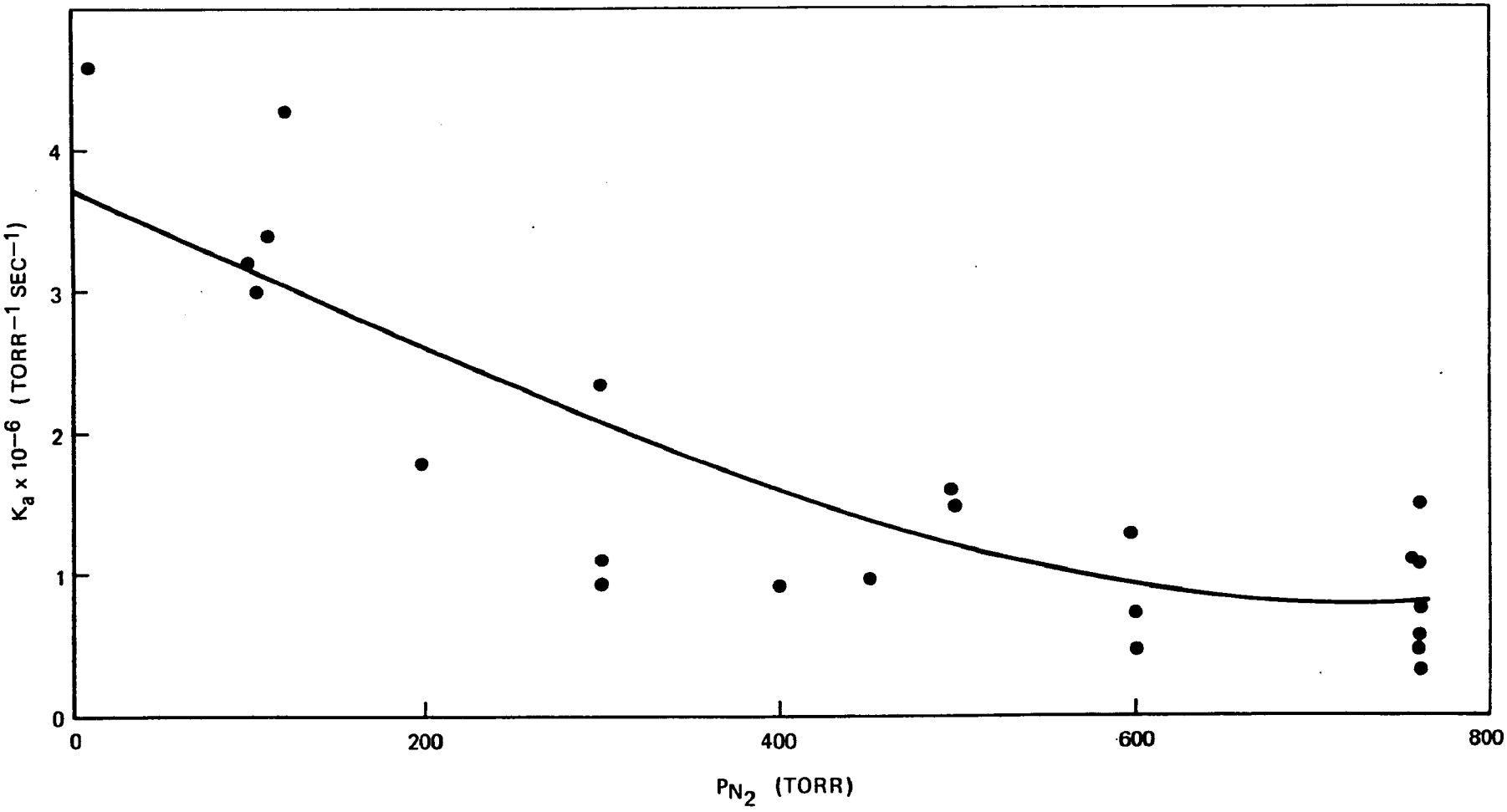

FIGURE 10. PRESSURE DEPENDENCE OF THE APPARENT RATE COEFFICIENT FOR QUENCHING OF SO_2 FLUORESCENCE AT 3105 Å BY N_2

The value of k_{N_2} was evaluated at each pressure using Equations 8 and 9 and the rate coefficients given in Table 1. All of such calculated values of k_{N_2} are shown in Fig. 10 as a function of the added nitrogen pressure. That k_{N_2} is pressure dependent is immediately apparent and X_a^{-1} is plotted against p_{N_2} in Fig. 11 for those runs in which results were obtained at more than two pressures. Assuming that Fig. 11 indicates the validity of the model from which Eq. 11 was derived, these results show that the ratio of the Raman scattered component intensity to that of the zero N_2 pressure fluorescence scattered component to be independent of the laser line wavelength in the region between 2997.8 Å and 3004 Å. The value of this ratio is seen to be $2.4 \pm 0.9 \times 10^{-3}$ and the value of k_{N_2}, calculated from the zero pressure intercepts of these curves, is found to be $3.8 \pm 0.6 \times 10^{-6}$ sec^{-1} $torr^{-1}$, which is to be compared to Metee's value of 2.7×10^{6} sec^{-1} $torr^{-1}$. Measurements were also taken with the fluorescence cell heated to 200°C as measured by a chromel-Alumel thermocouple. As at room temperature, the quenching coefficient calculated by Eq. 9 exhibited a dependence on the nitrogen pressure. However, the scatter in the data was too great to draw any useful information from it (Ref. 13).

Discussion

The results obtained above can be used to calculate an upper bound for the magnitude of the Raman scattering cross-section for radiation initially of wavelength 3000 Å scattered by SO_2 at wavelength 3105 Å. From the absorption coefficient data given in Fig. 1, the absorption cross section at 3000 Å, σ_a, is calculated to be 5.9×10^{-19} cm^2. Were all absorbed energy to be re-emitted unquenched as fluorescence at 3105 Å, the cross section per steradian for fluorescent scattering at 3105 Å would be 4.7×10^{-20} cm^2 sr^{-1}. As indicated by Fig. 2, only a fraction of the energy is emitted at this wavelength, and this cross section must therefore be considered an upper bound to the true value. The experimentally measured ratio of Raman scattering to unquenched fluorescence at 3105 Å was $2.4 \pm 0.9 \times 10^{-3}$. Proceeding as in Section IIB, the value of this ratio can be expressed as follows

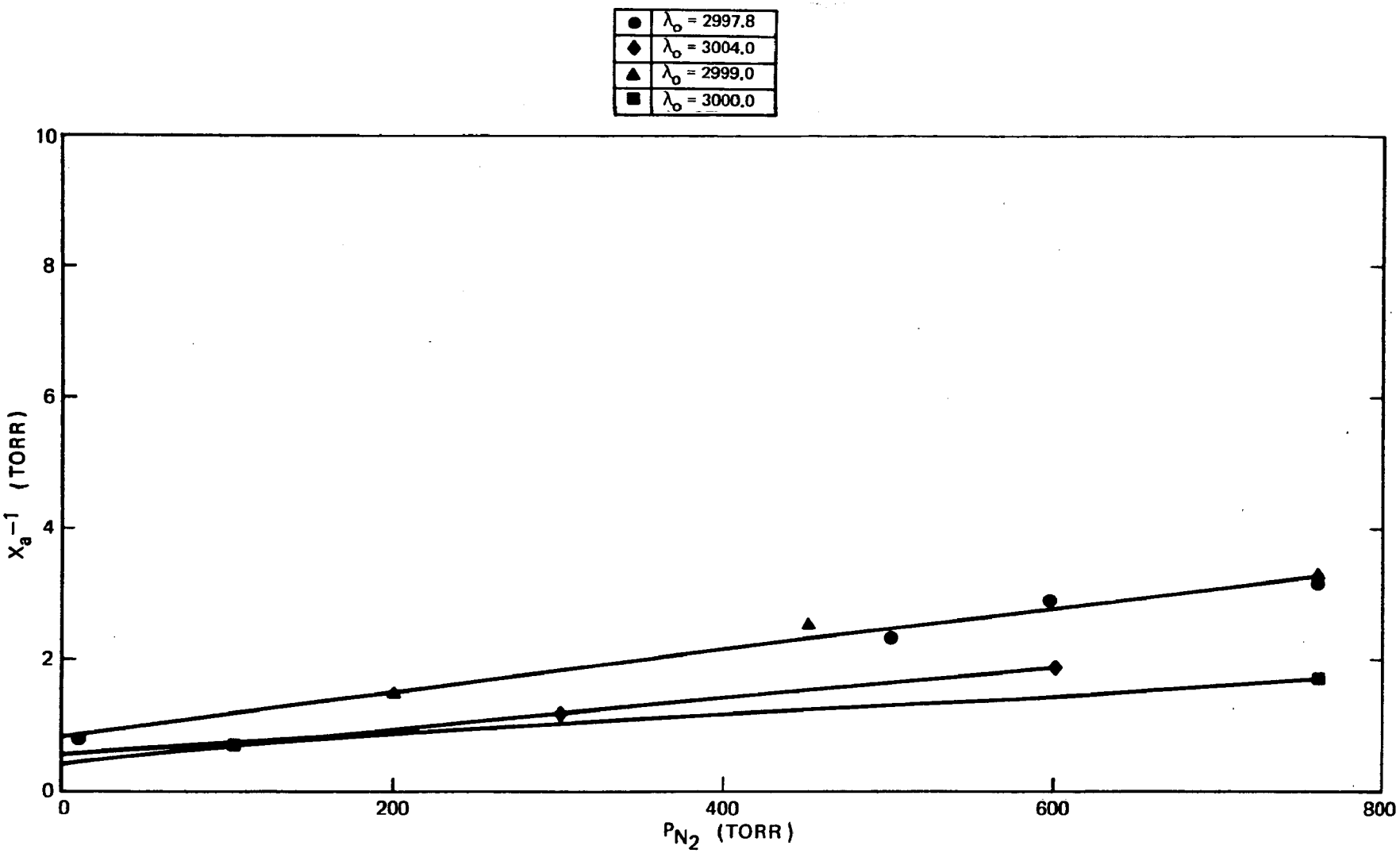

FIGURE 11. PRESSURE AND LASER WAVELENGTH DEPENDENCE OF X_a^{-1}

$$\frac{I_R}{I_F^o} = \frac{\sigma_R \, k_{SO_2} \, p_{SO_2}}{\sigma_a \, r_r} \qquad (13)$$

Where σ_R is the Raman scattering cross section, and the other quantities have been defined previously. For the data presented in Fig. 11, the value of p_{SO_2} was typically 0.4 torr, and the calculated value of σ_R is therefore seen to be 7.7×10^{-25} cm^2 sr^{-1}. The magnitude of this cross section can be calculated, ignoring all resonance effects, from the cross section measured for argon ion laser radiation at 5145 Å (Ref. 14) by simply assuming that the cross section increases as ν_s^4. The result of this calculation is 1.2×10^{-29} cm^2 sr^{-1}, inferring a factor of about 6×10^4 as the upper bound for the degree of enhancement of the cross section as a result of resonance effects. As mentioned in Section IIC, the magnitude of enhancement can be as high as 10^6, and, considering the weakness of the assumption concerning the size of the fluorescence scattering cross section, the magnitude of the enhancement inferred from the measurement is not unreasonable.

The impact of the experimental results upon the feasibility of using resonance scattering for the remote detection of SO_2 in stationary source emissions is considerable. The experimental results indicate that, in the absence of foreign gas quenching effects, a fraction of the incident laser intensity at 3000 Å is scattered by the Raman effect at 3105 Å. For 0.4 torr SO_2, the size of the fraction is 2.4×10^{-3} when the measurements are made over a 24 Å wide interval and is expected to increase as this interval size is decreased. In addition, the size of this fraction exhibits negligible dependence on the incident laser wavelength over a six angstrom unit range about the SO_2 absorption line at 3000 Å. The size of this fraction increases with pressure as the fluorescence component becomes quenched. The ratio of Raman signal to fluorescence is about 1.8 at atmospheric pressure, causing the scattered signal to be nearly three times as large as that expected in the absence of Raman scattering. As shown in Section IIA, an error as large as 30% in the measured scattered intensity can occur because

of composition variation in the gas mixture being analyzed if the intensity is due completely to fluorescence. The presence of the Raman component reduces this error to about 11%, and, as mentioned above, this error is decreased still further as the wavelength interval of the measurement is decreased. Therefore, the presence of the Raman component significantly increases the magnitude of the scattered signal and also its validity as a measure of the SO_2 concentration in the gas being analyzed.

Several questions do remain with respect to the validity of the light scattering technique as an SO_2 concentration probe. Although some measurements were taken with the gas sample at 200°C, no information was gained with respect to the effect of temperature upon the Raman to unquenched fluorescence ratio. Temperature effects, if any, are likely to arise from the temperature dependence of the quantity $d_{n''}$ in Eq. 6, and these effects should be investigated. Furthermore, the problems concerning the signal scattered inelastically by soot, fly ash, or other components present in a smoke stack plume have not been addressed in this study.

Section IV Conclusions and Recommendations

A. Introduction

In this section the experimental results described in Section III are utilized to evaluate the feasibility of using resonance scattering at 3000Å from SO_2 for the remote detection of that molecule. In particular, the following subjects are addressed: 1) The experimental results are utilized to calculate E_ℓ, the laser pulse energy necessary to make possible the detection of X parts per million SO_2 in a volume ℓ cm long at a distance L km from the laser-detector unit, and it is found that a laser delivering one mJ at 3000Å in a pulse one microsecond long is sufficient to allow detection of 100 ppm SO_2 distributed over a meter wide stack from a distance of 0.9 km. This pulse energy is well within present laser technology. 2) The extent to which quenching of ordinary fluorescent scattering degrades the accuracy of the measurement is reviewed and laboratory scale programs suggested to ascertain whether under field conditions the magnitude of the Raman signal is so much larger than the fluorescence signal that fluorescence quenching in no way degrades the accuracy of the measurement. 3) By considering the solar radiance present at 3000Å it is found that the interference to the measurement caused by scattered sunlight is negligible. 4) Some recently available results concerning fluorescent and Raman scattering by particulates are discussed, and these results are found to infer that such scattering may be a limitation to the usefulness of resonance scattering as an SO_2 concentration probe, thereby giving rise to the need for field tests in which the degree of scattering at 3000Å from plumes free of SO_2 is determined.

B. Lasers For SO_2 Detection

The results reported above may be utilized to calculate E_ℓ the laser pulse energy necessary to make possible the detection of X parts per million SO_2 in a volume ℓ cm long at a distance L km from the laser detector unit. This

quantity is expressed simply for suitably short pulses of width T_ℓ and low background signal level by the following equation which expresses the condition of equivalence between the magnitude of the laser power scattered by the SO_2 sample and returned incident to the detector and the detector's noise-equivalent power, P_{nep}, the power incident on the detector necessary for unity signal-to-noise ratio:

$$\frac{P_{nep}}{n} = \frac{E_\ell}{T_\ell} \eta_T \eta_Q \eta_{T'} \eta_c \eta_{opt} (\eta_F + \eta_R) \qquad (14)$$

For the photomultiplier, detector and laser pulse width used in this study the value of P_{nep} is calculated to be 3.5×10^{-12} W(Ref. 15). In Eq. 14, the quantity n is the number of pulses involved in the measurement, and the various η's are efficiencies and are defined as follows: The quantities η_T and $\eta_{T'}$ are the fractions of the incident laser radiation and the detected scattered radiation respectively transmitted through the atmosphere and are given by $\exp(-\alpha_i L)$ and $\exp(-\alpha_s L)$ where α_i and α_s are the atmospheric attenuation coefficients at the incident and scattered wavelengths (Ref. 16). The ratio of the scattered detected photon energy to that of the incident photon is given by η_Q. The fraction of the 4π steradian solid angle about the irradiated sample which is subtended by the detector is given by the ratio of the radiation collector area, assumed to be 0.1 m^2, to $4\pi L^2$ and is represented in equation 14 by η_c. The transmittance of the detector and collecting optics is given by η_{opt} and assumed to be 50% in the results given below. If the irradiated sample is not optically thick at the laser wavelength, the absorption and fluorescent scattering efficiency is given by

$$\eta_F = \chi N \sigma_a \ell \eta_{FE} \eta_\lambda \qquad (15)$$

where N is the gas density in the sample, σ_a the SO_2 absorption cross section η_{FE} the fluorescent efficiency given by equation 4, and η_λ the fraction of the fluorescence which falls within the wavelength limits of the detector, assumed to be 2% here. Finally η_R, the Raman scattering efficiency, is given by

$$\eta_R = X\eta\,\sigma_R \ell \tag{16}$$

where σ_R is the Raman scattering cross section, and it is assumed that the wavelength limits of the detector are wider than the laser linewidth. Figure 12 presents E_ℓ as a function of L and the product of X and ℓ for a measurement involving 100 laser pulses with η_{FE} calculated using the 300°K data given in Table 1. It is seen that a laser pulse of one mJ at 3000Å is sufficient to allow detection of 100 ppm distributed over a one meter wide stack at a distance of 0.9 km. For a pulsed dye laser, a second harmonic conversion efficiency of as high as 10 percent (Ref. 17) has been obtained, and between 5700Å and 6300Å more than a Joule of dye laser output can be achieved (Ref. 18) making the above-mentioned millijoule of laser output at 3000Å within the state of the art in tunable laser sources.

C. The Problem of Quenching

In Section II B the effect that fluorescence quenching has on the accuracy of the determination of SO_2 concentration from detected fluorescent scattering was considered in some detail. It was found that an error as large as 30% was generated by stack-to-stack variation in the concentration of effluents other than SO_2. In addition it was pointed out that the SO_2 fluorescent quenching rate coefficients can be expected to depend on the temperature so that stack-to-stack variation in the latter quantity provides another source of error. In Section II C, the properties of the Raman effect were discussed, one of these properties being immunity to quenching, and the experimental results of Section III revealed the presence of a large resonance Raman scattering component capable of reducing the above mentioned sensitivity to gas composition by at least a factor of three. This sensitivity is obviously proportional to the ratio of the fluorescence scattering component to the Raman component,

$$\eta_F/\eta_R = \sigma_a\,\eta_{FE}\,\eta_\lambda/\sigma_R \tag{17}$$

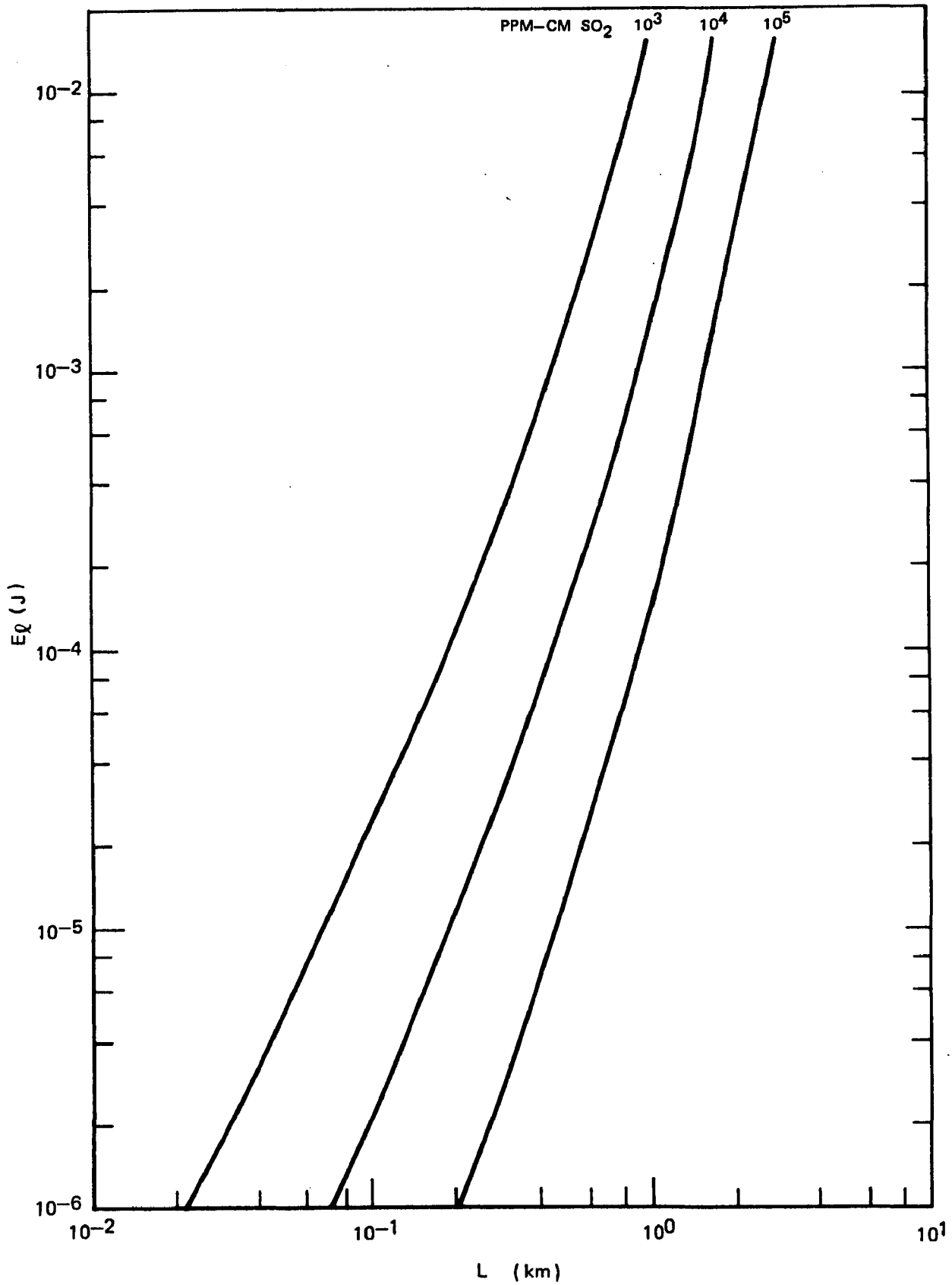

FIGURE 12. LASER PULSE ENERGY NEEDED TO DETECT SO_2 AS FUNCTION OF DISTANCE L FROM SAMPLE

and is smallest under conditions where the fluorescent efficiency is smallest or the Raman scattering cross section is largest. If it were known that, for the temperatures typically found in stationary sources, the fluorescent efficiency were substantially smaller than the value calculated from the 300°K data shown in Table I, the composition and temperature sensitivity described above may well be negligible. On the other hand, if the Raman scattering cross section can be increased substantially by, for instance, tuning the wavelength of the incident laser radiation to a different maximum in the SO_2 absorption spectrum this sensitivity may again by made negligible. For this reason, the temperature sensitivity of η_{FE} and the wavelength sensitivity of σ_R are the subjects of discussion of this section.

As shown by Eq. 4, the value of η_{FE} is determined by the magnitude of the fluorescence quenching rate coefficients k_i each of which can be thought of as the average value of the product of the relative speed v_r between the SO_2 molecule and the quenching species and the quenching cross section σ_a for that species, the average being taken over all values of the relative speed. At higher temperature the probability of collisions involving larger values of v_r increases so that, were σ_q to be independant of v_r, the value of k_i would be expected to increase as the square root of the temperature (Ref. 19). However such behavior is never observed as the value of σ_q often exhibits a quite complicated dependence on v_r. As an example, consider the quenching of 4.3 μm emission from vibrations excited CO_2 by N_2 (Ref. 20). The quenching is accomplished by either of two mechanisms. The first involves the transfer of vibrational energy from CO_2 to N_2, and the second involves the redistribution of vibrational energy within the CO_2 molecule as a result of the collision with the N_2 molecule. The simple treatment described above predicts a 40% increase in the quenching rate coefficient as the gas temperature is increased from 300°K to 600°K. In practice, however, the 4.3 μm quenching rate is observed to increase by order of magnitude for the latter of the two mechanisms described above and to <u>decrease</u> by 30% for the former. There is no reason to believe that the temperature behavior of the quenching

rate for electronically excited SO_2 is any less complicated, a fact which points out the necessity of actually measuring these rates rather than estimating them from simple physical arguments.

As discussed above, an alternative to determining the magnitude of η_{FE} at elevated temperatures is to investigate whether σ_R is substantially larger at some maximum in the SO_2 absorption spectrum other than the G line on which measurements were made in Section III. As was the case for calculating the temperature dependence, making an a priori estimate of σ_R and its variation from one SO_2 absorption line to another is extremely difficult. As indicated from equation 6, such a calculation requires detailed information of the shape of the potential energy curves for the upper and lower electronic levels, and this information is itself not easily obtained. Instead, the value of σ_R must be obtained experimentally for several SO_2 absorption lines in order to ascertain whether its magnitude varies significantly from one line to another. In addition, reference to figure 5 reveals that in the resonant Raman effect scattering often occurs at frequency displacements other than that corresponding to the ordinary Raman effect. Thus, the most comprehensive laboratory measurement involves determining η_F/η_R at several frequency displacements from the incident laser frequency as well as several incident laser frequencies.

D. The Problem of Background Radiation

In practice, determination of the SO_2 concentration in stack plumes will occur with the sky being present as a background to the plume and thus acting as the main source of background radiation to the detector. The properties of the sky as a radiance source are presented by Platt (Ref. 21) where it is seen that the radiance, N_λ, of the sky on a day of excellent visibility is about 10^{-6} W/(cm^2 μm steradian) at 3100Å. In a manner similar to that used in Section IV B, the background power incident on the photocathode of the detector can be calculated from the expression

$$P_B = N_\lambda \eta_T \eta_{opt} \Omega'_c A_p' \Delta\lambda \qquad (18)$$

where $\Delta\lambda$ is the active wavelength interval of the detection system assumed here to be 10^{-4} μm. The quantity $\Omega'_c A_p'$ is the product of the solid angle subtended by the radiation collecting optic about the volume being analyzed, Ω_c', and the area of the image of the active detector surface projected on that volume A_p'. This product is equal to the product $\Omega_c A_p$ where Ω_c is the solid angle subtended by the collecting optic about the detector and is, for an f/10 optic, equal to 7.8×10^{-3} steradian, and A_p is the active detector surface, assumed to be one cm^2. The value of η_{opt} is taken, as before, to be 0.5 and η_T to be unity, rendering the calculated value of P_B an upper bound on the actual value. The calculated value of P_B is 3.9×10^{-13} watt which is an order of magnitude below the value of P_{nep} so that background radiation is not expected to be a problem at 3000Å.

E. Scattering From Particulates

It is unrealistic to expect that a typical smoke-stack under analysis will contain only molecular species. In practice it will also contain fly ash or other particulate species, and the question arises as to whether these particulates will scatter the incident laser radiation in such a way as to interfere with the determination of the SO_2 concentration. The light scattering properties of particulates found in stationary sources is the subject of a recently published report (Ref. 22) which considers both Raman and fluorescent scattering. Of the many particulates considered, only $CaSO_4$ displayed a frequency displacement, 1151 cm^{-1}, exactly equal to that of SO_2 although many other sulfates had displacements of the approximately the same size. Of perhaps greater interest was the finding of considerable broadband fluorescence from a number of particulate materials. This result indicates that scattering from particulates may indeed be an interference to the determination of the SO_2 concentration, but lack of detailed quantitative information

in reference 22 with respect to the magnitude of the fluorescent scattering cross sections prevents estimate of the magnitude of the problem.

F. Field Evaluation

The purpose here is to recommend a program for field evaluation of the resonant scattering technique at 3000Å as an SO_2 concentration probe. In Section IV C, it was pointed out that laboratory evaluation of this technique is still incomplete inasmuch as the temperature dependence of the fluorescent efficiency and the wavelength dependence of the resonant Raman cross section are yet to be determined. However, the results discussed in Sections IV B and E certainly indicate that the magnitude of the scattered signal is not a problem to the measurement but that scattering from particulates may be of sufficient importance to render any information obtained from further laboratory evaluation irrelevant. Therefore the most effective program of further investigation would seem to be actual field testing of this technique using a stationary source capable of emitting plumes whose composition can be controlled over a suitably wide spectrum. In such a program, the first step is to construct a laser and detection system capable of performing as predicted in Section IV B. Of particular importance in doing so is to ensure that the laser output be centered on the SO_2 absorption line and that the detector sensitivity by maximum at a wavelength exactly 1150 cm^{-1} displaced from the laser line. As the SO_2 G line is at 3000Å this may be accomplished by placing a narrowpass filter centered at 6000Å in front of the laser, and tuning the laser to maximize the power transmitted by this filter. A narrowpass filter centered at 3105Å would then ensure that the laser line center and detector sensitivity maximum differ by the desired amount. The actual field evaluation would involve first a series of tests at relatively short range in which the SO_2 concentration inferred from the scattering technique is compared with that measured by a standard technique for a wide range of effluent composition and temperature with special attention being paid to

the effect of the presence of particulates on the measurement. A second series of tests at longer ranges would then serve to verify the results of Sections IV B and E concerning the magnitude of the background signal and the dependance of the scattered signal upon the distance from the source.

REFERENCES

1. S. J. Strickler and D. B. Howell, J. Chem. Phys., 49 1947 (1968).

2. G. Herzberg: Molecular Spectra and Molecular Structure, (D. Van Nostrand Company, Inc., Princeton, New Jersey, 1950), Vol. I, pp. 194-202.

3. Ibid., pp. 212-280.

4. G. Herzberg, Op. Cit., Vol. III, pp. 511-512.

5. H. D. Metee, J. Chem. Phys., 49 1784 (1964).

6. H. D. Metee, J. Phys. Chem., 73 1071 (1969).

7. H. Eyring, J. Walter, and G. E. Kimball, Quantum Chemistry, (John Wiley and Sons, Inc., New York, 1944), pp. 118-123.

8. K. F. Greenough and A. B. F. Duncan, J. Am. Chem., 83 p. 555 (1961).

9. J. Behringer, pp. 168-223, Raman Spectroscopy, H. A. Szymanski, ed. Plenum Press, New York (1967).

10. S. H. Autler and C. H. Townes, Phys. Rev, 100 703 (1955) R. Gush and H. P. Gush, Phys. Rev. 6A 129, (1972).

11. P. P. Shorygin and T. M. Ivanova, Soviet Phys.-Dokl. 3 764 (1958).

12. M. E. Mack, Appl. Opt. 13 46 (1974).

13. It is noted that the scattered intensity was measured over a 24 $\mathring{A}$ wavelength interval, but that raman component occurs over an interval $\sim$ 0.5 $\mathring{A}$ wide corresponding to the full width of the laser line. Therefore, the value of the Raman to fluorescence intensity ratio over the smaller wavelength interval might be higher.

14. D. G. Gouche and R. K. Chang, Appl. Phys. Letters 18 579 (1971).

15. H. Kildal and R. L. Byer, Proc. IEEE 59 1644 (1971).

16. W. A. Baum and L. Dunkelman, J. Opt. Soc. Amer 45 166 (1955).

17. D. J. Bradley, J. V. Nicholas and J. R. D. Shaw, Appl. Phys. Letters 19, 172 (1971)

18. C. M. Ferrar, Rev. Sci. Inst. 40, 1437 (1969)

19. R. D. Present, "Kinetic Theory of Gases" (McGraw-Hill Book Company, Inc. New York, 1958) pp 143-145

20. R. L. Taylor and S. Bitterman, Rev. Mod. Phys. 41, 26 (1969)

21. W. K. Platt, "Laser Communication Systems" (John Wiley and sons, New York 1969) p. 121

22. M. L. Wright and K. S. Krishnan, "Feasibility Study of In-Situ Source Monitoring of Particulate Composition by Raman or Fluorescence Scatter" Environmental Protection Agency Report EPA-R2-73-219, June 1973.

BIBLIOGRAPHIC DATA SHEET	1. Report No. EPA-650/2-74-020	2.	3. Recipient's Accession No.
4. Title and Subtitle: Feasibility Study of the use of Resonance Scattering for the Remote Detection of SO_2			5. Report Date: January 1974 6.
7. Author(s): Michael C. Fowler and Paul J. Berger			8. Performing Organization Rept. No. N921480-18
9. Performing Organization Name and Address: United Aircraft Research Laboratories, East Hartford, CT 06108			10. Project/Task/Work Unit No. 11. Contract/Grant No. EPA 68-02-0656
12. Sponsoring Organization Name and Address: Environmental Protection Agency, NERC, CPL, Research Triangle Park, NC 27711			13. Type of Report & Period Covered: Final Report 14.

15. Supplementary Notes

16. Abstracts

An analytical and experimental investigation has been carried out to determine the feasibility of using the scattering of ultraviolet radiation by SO_2 as a probe of the concentration of that molecule in stationary source emissions. Both ordinary fluorescence and resonant Raman scattering were considered and experimentally it was found that the latter component was present in the scattered radiation with sufficient magnitude to reduce significantly the degrading effect that ordinary fluorescent quenching has on this scattering technique. Further analysis revealed that current state-of-the-art dye lasers deliver sufficient ultraviolet pulse energy to permit SO_2 concentration determination in practical situations but that fluorescent scattering from particulates presents a possible constraint to the validity of this technique. A field program is recommended to investigate the latter.

17. Key Words and Document Analysis. 17a. Descriptors

Sulfur Dioxide
Lasers
Light Scattering
Raman Spectroscopy
Resonance Absorption
Resonance Scattering
Fluorescence
Air Pollution
Airborne Wastes
Exhaust Emissions
Optical Detection
Ultraviolet Detection
Remote Sensing
Signatures

17b. Identifiers/Open-Ended Terms

Resonant Raman Scattering
Dye Lasers
Tunable Lasers

17c. COSATI Field/Group 7B 20E

18. Availability Statement	19. Security Class (This Report) UNCLASSIFIED	21. No. of Pages 51
	20. Security Class (This Page) UNCLASSIFIED	22. Price